

RESEARCH ARTICLE

Sentinel-1 Data to Support Monitoring Deforestation in Tropical Humid Forests

Christian Vargas^{1*}, Takuya Itoh², Takahiro Koide³, Kazuyo Hirose⁴, Fernando Regal¹, Michinori Yoshino⁵, Hiroaki Okonogi⁶, Kelly Salcedo Padilla⁷, Nataly Valencia Vento⁷, Corina Navarrete Macedo⁷, Elvira Gomez Rivero⁷

¹Independent consultant, Peru

²Remote Sensing Technology Center of Japan, Japan

³Kokusai Kogyo Co. Ltd, Japan

⁴Japan Space Systems, Japan

⁵Nippon Koei Co., Japan

⁶Japan International Cooperation Agency, Japan

⁷National Forest and wildlife service, Peru

*Corresponding author: Christian Vargas: geocvargas@gmail.com



Citation: Vargas C., Itoh T., Koide T., Hirose K., Regal F., Yoshino M., Okonogi H., Padilla K.S., Vento V.N., Macedo C.N., Rivero E.G. (2021) Sentinel-1 Data to Support Monitoring Deforestation in Tropical Humid Forests. *Open Science Journal* 6(4)

Received: 20th January 2021

Accepted: 27th October 2021

Published: 23rd November 2021

Copyright: © 2021 This is an open access article under the terms of the [Creative Commons Attribution License](#), which permits unrestricted use, distribution, and reproduction in any medium, provided the original author and source are credited.

Funding: The author(s) received no specific funding for this work

Competing Interests: The authors have declared that no competing interests exist.

Abstract:

In recent years, methodologies for deforestation detection that use satellite data have been developed, primarily using optical data, which cannot detect deforestation in the presence of clouds. In this paper, we discuss a methodology developed to detect deforestation using Sentinel-1 data and that aims to complement typical early warning system based on optical satellite images such as one the Peruvian Government employs. The methodology was applied in three pilot areas in the tropical humid forest of Peru. Sentinel-1 data were acquired in Interferometric Wide Swath (IW) mode and VH polarization. We use a Gamma-Map filter to reduce the speckle noise, and the average of 3 chrono-sequentially continuous images to reduce the multi-temporal variation of the forest backscattering. This produced 6 time series for each pilot area. For the detection of deforestation, we used an algorithm based on the difference and ratio between the images before and after deforestation. The accuracy assessment revealed a user's accuracy greater than 95%. We also made a multitemporal comparison between our results and the early warning tropical forest loss alerts that use only Landsat data, which showed that until the end of the study period 33.26% of the deforestation we detected was not detected by the early warning alerts that use Landsat data.

Keywords: Detection of deforestation, Early warning alerts, Sentinel-1, C-band SAR, Humid tropical forest, Peru

Introduction

The land-use change due to deforestation is one of the main causes of the emission of carbon dioxide into the atmosphere.

In Peru, the economic sector that contributes the greatest amount of emissions corresponds to the land use, land-use change and forestry sector (LULUCF), with 51% of total emissions [1], mainly due to the deforestation of Amazonian rainforests.

The use of satellite sensors has allowed the development of early warning systems that detect deforestation, making it possible for competent institutions to evaluate the legal status of deforestation, and take corrective measures that lead to a timely intervention to stop deforestation in areas that don't have land-use change permits [2], while helping to deter future unauthorized land-use changes [3].

Satellite sensors with high temporal resolution and low spatial resolution, such as the Moderate Resolution Imaging Spectroradiometer (MODIS), are used to detect changes in forest coverage almost in real-time. Unfortunately, the spatial resolution of these satellite sensors doesn't allow them to detect small-scale deforestation [4-7]. The detection of small-scale deforestation can be detected with the use of Landsat Enhanced Thematic Mapper Plus (ETM+) sensor data onboard Landsat 7 and the Operational Land Imager (OLI) sensor data onboard Landsat 8 in methodologies such as the one developed by the Global Land Analysis and Discovery Laboratory (GLAD) of the Geographical Sciences Department of the University of Maryland [8] and the one developed by the National Program of Forest Conservation for Climate Change Mitigation (PNCBMCC) of the Ministry of the Environment of Peru [2]. Landsat data can detect deforestation events or forest cover disturbances of less than 0.09 ha and with a potential frequency of 8 days [2,8]. The downside of using Landsat data is the presence of clouds, especially in the humid season. Figure 1 shows the loss of tropical humid forest cover in Peru that occurred in 2018 and was detected by GLAD and the PNCBMCC (Geobosques). These figures were calculated on the primary forest layer of the year 2017 developed by PNCBMCC. Data clearly show that in the humid season the detection of forest loss is very limited and that probably many deforestation events that occurred in such season were only being detected months later in the dry season. This limitation is critical when we plan to use this data as an early warning system since this requires to detect deforestation in the shortest possible time.

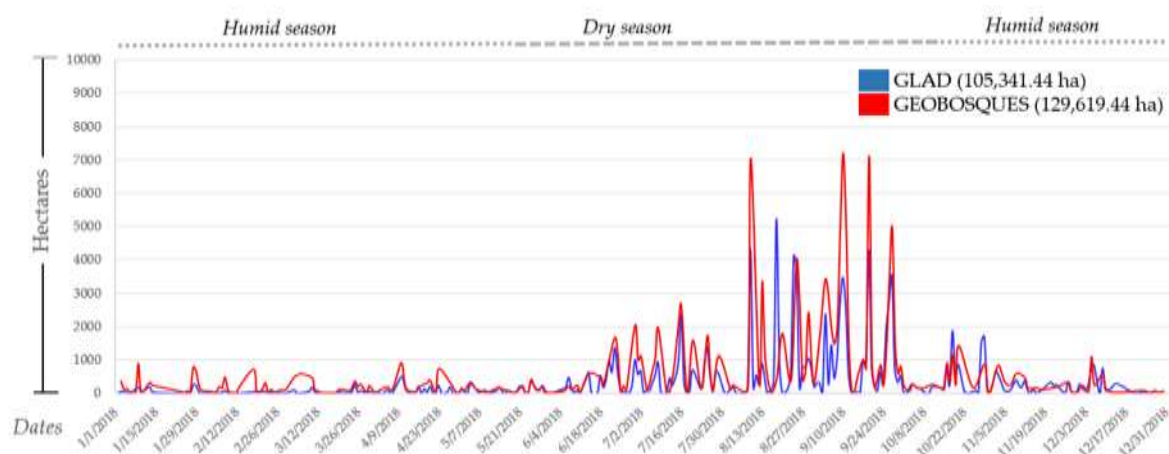


Figure 1. Comparison of forest cover loss detected by GLAD and GEOBOSQUES

The Synthetic Aperture Radar (SAR) data is an alternative to detect deforestation in areas with high cloud presence because the wavelength of the microwaves is able to penetrate clouds, rain, haze, and smoke [9]. The use of SAR data in the detection of deforestation of tropical forests has already been studied [10-15], and there are also studies where they combine the use of optical data and SAR for the detection of deforestation [16-18]. In November 2016, the first early warning system for deforestation using SAR (L-band) data called JICA - JAXA Forest Early Warning System in the Tropics (JJ - FAST) was launched. This system uses PALSAR-2 data in its ScanSAR mode, generates alerts every 1.5 months and has the capability to detect at least a 3 ha-sized deforested area [19], making it a very successful system in countries such as Brazil [20,21]. Currently, Peru uses this technology to fill the information gap left by methodologies that use optical data in the humid season. However, the minimum detection area achieved by JJ-FAST is not enough, because in recent years in Peru more than 70% of deforestation has occurred in areas smaller than 5ha [2,22]. Recent studies have shown that Sentinel-1 data can detect forest loss that is smaller than 5ha. Reiche et al. [23] used Sentinel-1 data in the detection of forest cover loss in the Riau province in Indonesia, to detect deforestation using a probabilistic method based on Bayesian classification, and obtained high user's and producer's accuracy. However, deforestation due to the expansion of agroindustrial plantations (oil palm and others) predominates in the province of Riau, and this type of deforestation is characterized by covering large areas, where normally the deforested area is free of residues (trunks of trees, bushes or stems) on its surface, which makes the difference between the backscattering of the forest and that of the deforested area be detected easily. In Peru, the reality is different, since deforestation of small and medium scale predominates, and often this deforestation leaves residues on its surface, generating a backscattering similar to that of the forest and making detection of the deforestation more difficult. Recently, Bouvet et al [15] used Sentinel-1 data in ascending and descending orbital nodes to detect deforestation in an area within the San Martin Region in Peru and used the shadows generated between the forest and the deforested area to establish deforested areas. The results were promising, however, the thresholds needed to have an automated method for detecting deforestation with high accuracy still need to be studied. The methodology proposed by Bouvet et al [15] was also used with optical data to improve the detection of deforestation [24]. Another experience in combining Sentinel-1 and Landsat data for the detection of

forest changes was carried out in Myanmar, where the detection of changes using Sentinel-1 had a user's accuracy of 75.5% [25]. Peru was one of the first countries in the world to access GLAD's early warnings alerts, and therefore it has a few years of experience in the use and application of this information. A recent study by Global Forest Watch [26] showed that early warning alerts are primarily used to investigate illegal activities, monitor natural protected areas, enforce land rights and conservation agreements with native communities, and raise awareness of illegal deforestation. The National Forest and Wildlife Service of Peru (SERFOR) identifies potential illegal deforestation greater than 1 ha.

The deforestation information detected is verified using Sentinel-2 images. SERFOR generates a report for each area with signs of potential illegal activity and sends it to the competent institutions so that they can take immediate action and prevent the advance of deforestation. Other institutions like The Peruvian Service for Natural Protected Areas (SERNANP) use the information from early warnings alerts to monitor unauthorized land use changes within national parks. Before conducting a field visit, institutions verify whether the detection is correct using Sentinel-2 images, other satellite images with better spatial resolution have a higher cost that cannot be covered by government institutions. Sentinel-2 is a good alternative to verify data before going to the field, but weather conditions are not always optimal and oftentimes there are no Sentinel-2 images available. When this occurs, institutions have to send personnel to verify deforestation in the field, which represents an investment of time and money, and verifiers can take several days to reach a verification point due to the lack of roads; all this effort can be overshadowed when they confirm a false positive. For these reasons, it is important for users to have confidence in early warning data.

The methodology we have developed aims to complement Peru's early warning system based on Landsat images. This methodology is not aimed at producing accurate estimates of deforestation but to provide a simple and easily applicable approach that can be replicated by any user seeking a more exhaustive detection than what systems based on optical data can provide in the wet or rainy season, and thus support the implementation of REDD+ activities. Considering that field verifications require time and money, we have prioritized having a high user accuracy, sacrificing producer accuracy. Lastly, to demonstrate the usefulness of our methodology in the wet or rainy season, we compared our results to those obtained with early warnings that use Landsat data.

Materials and methods

Study area

The study was developed in 3 pilot areas within the tropical humid forest of Peru (see figure 2) [27]. The pilot areas are located on important deforestation fronts within the San Martín, Ucayali and Madre de Dios regions, which are considered as part of the regions with the highest deforestation in Peru [28]. The cloud coverage in these areas is different, San Martín is characterized by having less availability of optical images with a low percentage of clouds cover than Ucayali or Madre de Dios, but in all of the cases, the availability of optical images with a low percentage of cloud cover is very limited. The extent of the pilot areas can be found in Table 1.

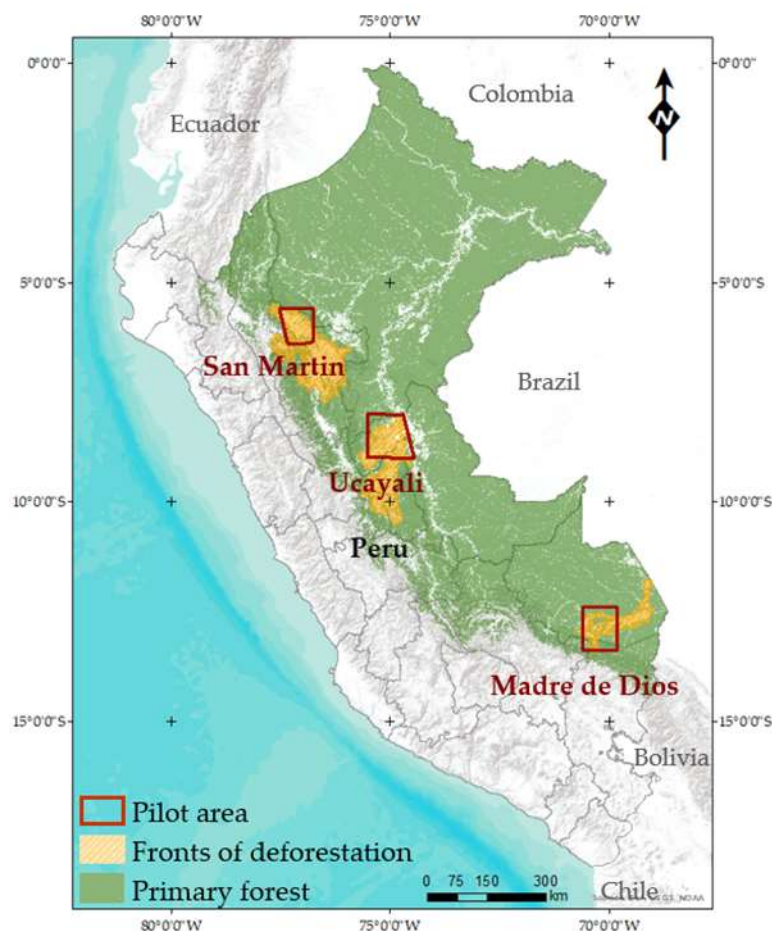


Figure 2. Location of pilot areas

The San Martín pilot area is part of the deforestation front of the same name, where large scale as well as small scale agriculture predominates [1]. It has flat topography in the central part and is mountainous on the sides. The Ucayali pilot area is part of the Federico Basadre - Marginal deforestation front, where agriculture of different scales and cattle ranching predominates [1]. Almost all the area has a flat topography but slightly mountainous in the western part. The Madre de Dios pilot area is part of the deforestation front called Tambopata - Manu, where artisanal gold mining [29,30] and cattle ranching [1] predominates. It is mostly flat with a mountainous area towards to the south.

The humid season in the tropical humid forest extends from November to May and the dry season does from June to October. In the dry season, methods for detection of deforestation that use optical sensors such as Landsat data tend to report a great of forest loss compared with the humid season; this is due to the greater availability of images with a low percentage of cloud presence in the dry season [2,8].

Data

Sentinel-1

The Sentinel-1 constellation is a part of the Copernicus Programme of the European Space Agency (ESA). Sentinel-1 collects C-band synthetic aperture

radar (SAR). For this study, we used 137 Sentinel-1 images (see table 2), downloaded through Google Earth Engine (GEE) at a spatial resolution of 20 m with VH polarization. The images were acquired in Interferometric Wide Swath (IW) mode and the Level-1 ground range detected (GRD) [31] was used. The collection of GRD scenes were processed to calculate the backscatter coefficient (σ^0) in decibels (dB) [32]. The repeat cycle of Sentinel-1 constellation around Peru is 12 days. The details of the images used for each pilot area are shown in Table 2.

Table 2. Details of Sentinel-1 images

Pilot Area	No. of images used		Pass	Relative Orbit
	Year 2017	Year 2018		
San Martin	14	18	Ascending	120
Ucayali	13	18	Ascending	120
Madre de Dios	26	18	Descending	127

Primary forest

The primary forest corresponds to the remnant primary forest layer for 2017. This layer was provided by the PNCBMCC and it is the same one used for the detection of early warnings of forest loss available in the Geobosques platform (<http://geobosques.minam.gob.pe/>). This layer was resampled at 20 m and cut following the same dimensions of the pilot areas.

Slope

To develop the slope map a Digital Elevation Model (DEM) of 30m from the Shuttle Radar Topography Mission (SRTM) was used. It was resampled and cut following the same dimensions of the pilot areas. To minimize the noise of the model, a low pass filter with a 7 x 7 window was applied. This information was used to create a layer of areas with slopes of less than 5° to mask moderate and high slopes which are revealed to contain a high presence of false positives by preliminary tests.

Reference data

Deforestation polygons obtained from the methodology developed in this study were compared with the tropical forest loss alerts data of the PNCBMCC. These alerts are generated based on data from the Landsat ETM+ and OLI sensors and can detect up to 25% size of forest cover loss within a Landsat pixel (30 m x 30 m). This data doesn't include the forest lost due to change in the course of the river [2] and are available on the Geobosques platform (<http://geobosques.minam.gob.pe/geobosque/view/descargas.php#download>).

Early warnings available in Geobosques have an average producer accuracy of 94.55% and an average user's accuracy of 94.54% [2], making it the most accurate forest loss data available for the tropical humid forests of Peru. For this reason, we have used this data as a reference to calculate the producer accuracy of our methodology.

Method

Processing of Sentinel-1 data

After testing different adaptive and convolution filters, we decided to apply the Gamma Map filter (1) with a 7 x 7 window to all the images. Figure 3, shows deforested areas in the Sentinel-2 image dated 09/07/2018 (a), a combination of Sentinel-2 images in RGB color (b), Sentinel-1 dated 09/05/2018 (c), and the same Sentinel-1 image with Gamma Map filter (d). In the Sentinel-2 image, it is possible to observe the deforested areas in light tones. In figure 3 (b), recent deforestation is shown in red and old deforestation (before 10/17/018) in light colors. However, these areas are not clear in the non-filtered Sentinel-1 image because the presence of deforestation residues on the surface (trunks of trees, branches or bushes) reflect backscattering signal to be captured by the sensor as the surrounding forests does. In figure 3 (d), deforested areas are easier to observe and are shown with a dark gray color; this is because the Gamma Map filter reduce the speckle noise and the signal coming from the residues and highlights the presence of soil or water (lower backscattering). This only occurs if the presence of soil or water in the deforested area is greater than the presence of residues.

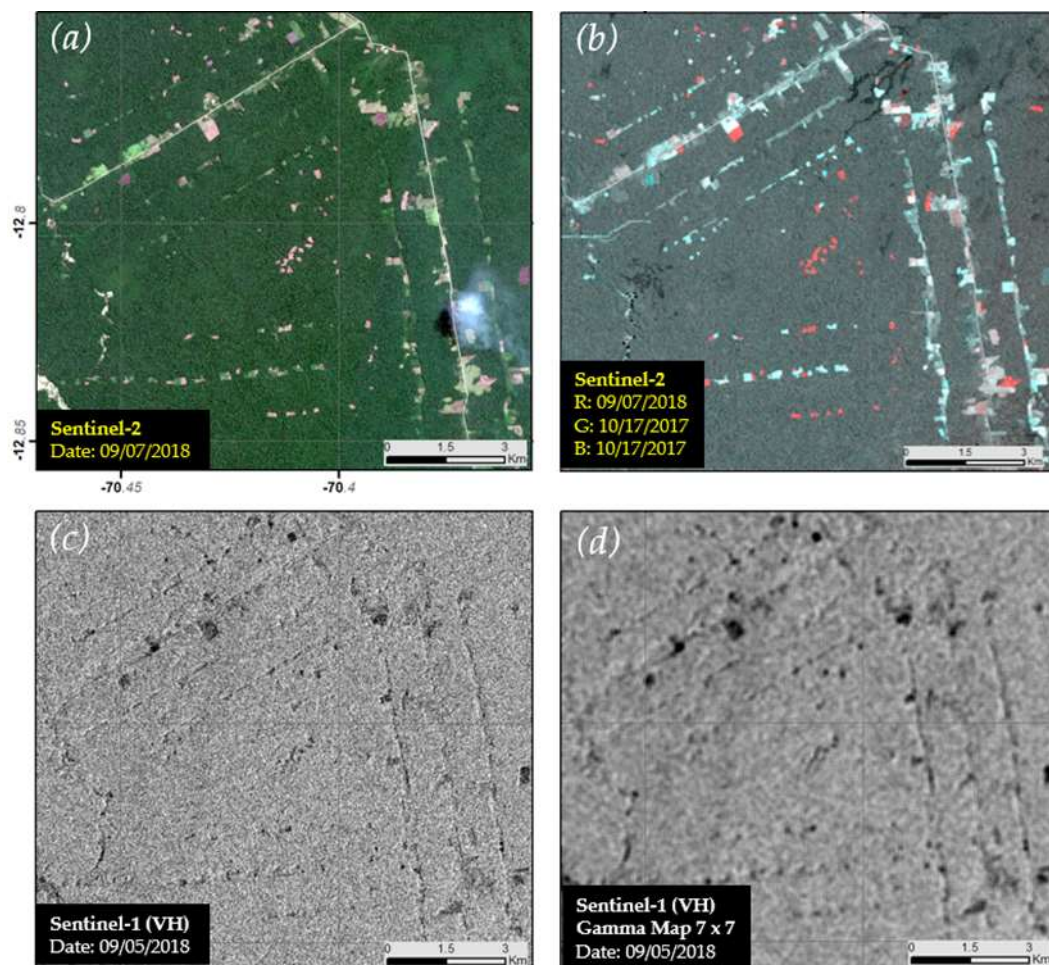


Figure 3. Deforestation events seen with Sentinel-2 (a), combination of Sentinel-2 images in RGB color (b), Sentinel-1 (c) and Sentinel-1 with Gamma Map filter(d).

The next step was to reduce the multitemporal variation of forest backscattering. Figure 4 (a) shows the highly fluctuating backscattering (between -13.87 and -14.62 decibels) at three random points in the forest observed in 18 consecutive Sentinel-1 images. To reduce this variance, we calculated the mean of three consecutive images. Figure 4 (b) shows the backscattering of the forest after calculating the mean of 3 consecutive images (The dates of the images used are indicated in table 3). The range of the calculated backscattering (between -14.11 and -14.45 decibels) is more than 50% smaller than that of the backscattering before the calculation. Reducing backscattering variance is an important step because in some cases this variance can be mistaken as deforestation events.

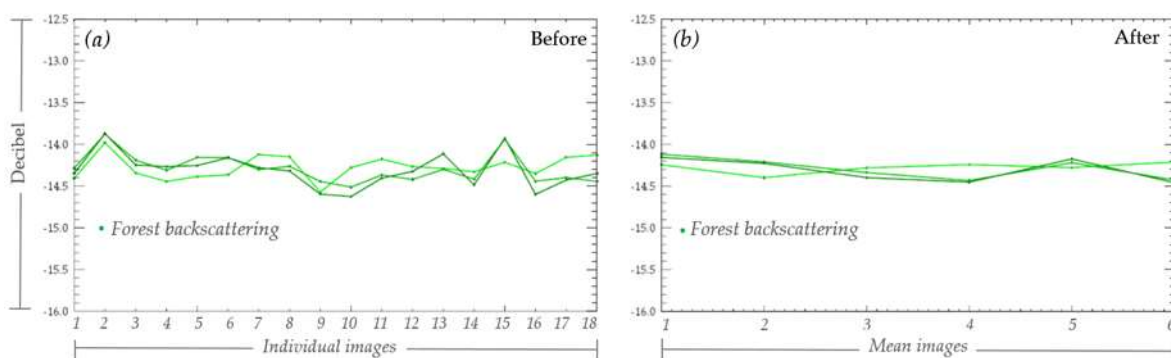


Figure 4. Variation of backscattering at three random points in the forest in individual images (a) and the mean of 3 images (b).

Then, using the 2018 images (18 for each pilot area), the means of three consecutive images were calculated, reducing the data to 6 new images, which from now on we will call as temporal series. Table 3 shows the dates of the images used to calculate the temporal series. In the best case, the detection interval is 36 days (12 days-repeat cycle x 3), however, this period can be extended when missing observations occurred. These temporal series were used to detect deforestation. In order to reduce the backscatter variation in the images taken before deforestation occurred, we decided to use the average of all available images for the year 2017 and were used as input images for the detection method (Table 2).

Table 3. Dates of Sentinel-1 images used to calculate the mean of three images in 2018.

Pilot Area	Humid Season			Dry Season			Temporal Series			
	Jan.	Feb.	Mar.	Apr.	May	Jun.		Jul.	Aug.	Sept.
San Martin	(19	12,24)	(08,20	01),(13,25	18),(30	12,24)	(06,18,30)	(11,23,	04)	6
Ucayali	(07,19	12),(24	08,20)	(01,13,25)	(18,30	12),(24	06,18),(30	11,23)		6
Madre de Dios	(08,20	13),(25	09,21)	(02,14,26)	(08,20	13),(25	07,19),(31	12,24)		6

Detection of deforestation

The detection of deforestation was done on areas that match the forest layer. The method used is based on simple mathematical operations, which have already been applied for the detection of deforestation using SAR data [14,34-36]. The following operations were used:

Method 1 = (Mean 2017 – mean of 3 images > 1.5)

Method 2 = (Mean 2017 / mean of 3 images < 0.9)

Method 1 uses the difference between images with a threshold greater than 1.5, and method 2 uses the ratio between images with a threshold less than 0.9. The thresholds were determined by visual verification, prioritizing the reduction of a false positive detection, and taking into account our objective of obtaining high user's accuracy. Both methods detect deforestation, but the main difference between the two methods is that method 1 is more sensitive to the forest loss due to changes in the course of rivers, as well as to certain shadows produced by the angle of the images. On the other hand, method 2 is more sensitive to problems like foreshortening and layover. Figure 5 shows the comparison of methods 1 and 2 in a sector of the pilot area of Madre de Dios, where it can be observed that method 1 detects more forest loss areas due to changes in the course of the river.

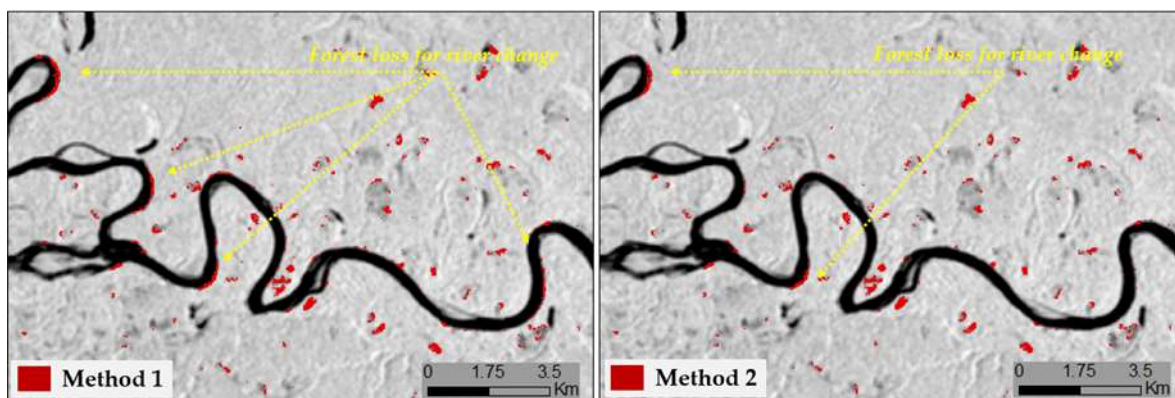


Figure 5. Comparison of detected deforestation obtained by method 1 and 2, respectively, in a sector of the Madre de Dios pilot area. The base image corresponds to the mean of 2017 Sentinel-1 images.

Figure 6 shows the comparison of methods 1 and 2 in a sector of the San Martin pilot area. It can be seen how method 2 detects areas with foreshortening and layover as deforestation.

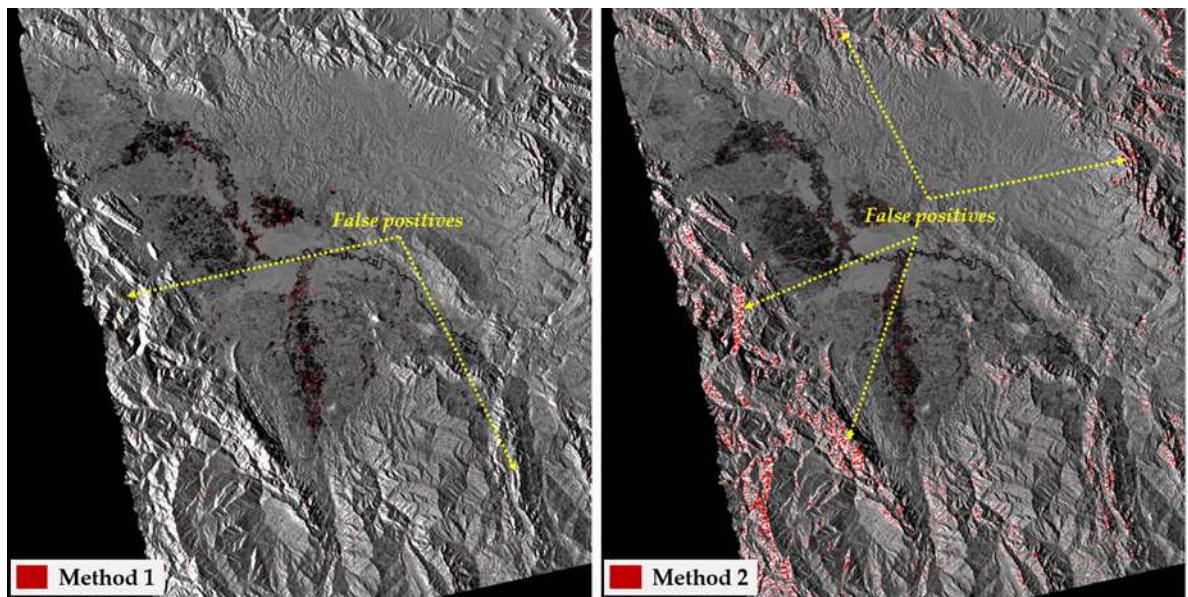


Figure 6. Comparison of detected deforestation obtained by method 1 and 2, respectively, in a sector of the San Martin pilot area. The base image corresponds to the mean of 2017 Sentinel-1 images.

Due to the high presence of false positives in mountainous areas due to foreshortening, layover and shadows, it was decided to detect deforestation in primary forests with slopes of less than 5° . Finally, while trying to achieve greater user's and producer's accuracy, method 1 and 2 were merged into one. To facilitate its application, the process of detecting deforestation was integrated in a binary decision tree. The result was preliminary deforestation for the time series available for each pilot area. As part of the post-processing, all groups of pixels <1 ha (25 pixels) were eliminated. The workflow followed is shown in Figure 7.

The software used for processing, detection and post-processing was ENVI®.

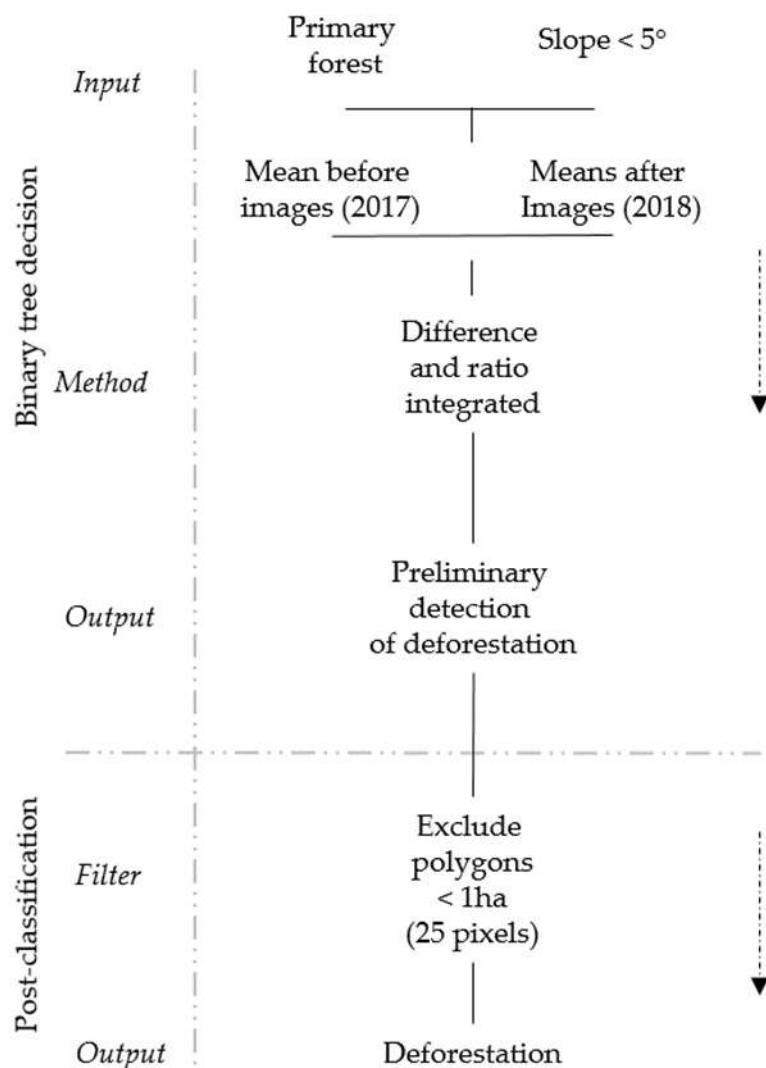


Figure 7. Workflow followed for the detection of deforestation.

Verification and evaluation of the accuracy

To evaluate the accuracy of results, all deforestation polygons detected were visually verified with satellite images from sensors on board the Sentinel-2 mission and the Landsat 7 and 8 satellites; these images were taken between January and September 2018. To maintain the transparency of the results, the verification was carried out by 3 people from the Satellite Monitoring Unit of SERFOR, where the third person solved discrepancies of the other two interpreters.

Polygons with more than 50% of deforestation were considered as correct detections, and the same criterion was applied for forest loss due to changes in the course of a river.

Figure 8 shows an example of verification of the deforestation polygons detected based on a Landsat OLI image dated 07/16/2017.

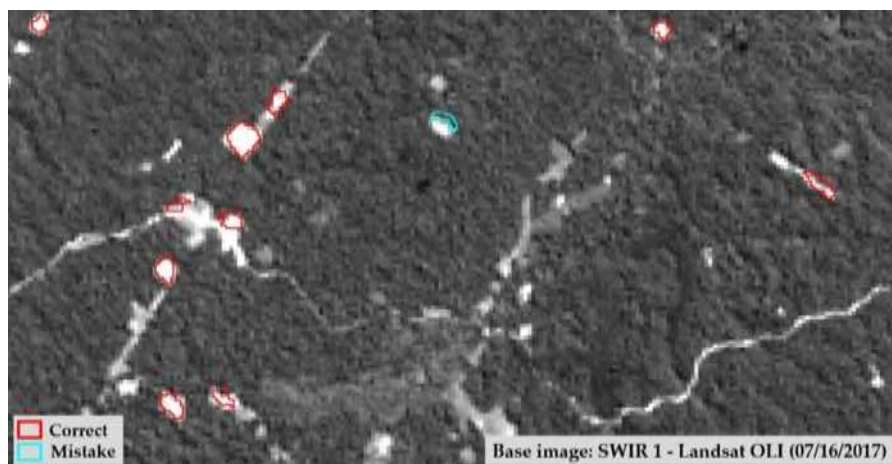


Figure 8. Example of interpretation of deforestation polygons.

User's accuracy and producer's accuracy was obtained using the following formulas:

- User's accuracy = Deforestation correctly detected / Total deforestation detected
- Producer's accuracy = Deforestation correctly detected / Deforestation > 1 ha detected by Geobosques

The early warnings alerts detected from January 2018 until the closest date of each temporal series are accumulated, respectively. The forest loss due to changes in the river courses and the false positives obtained with our methodology were excluded in the calculation of producer's accuracy because Geobosques does not include this type of forest loss in its analysis.

Additionally, to assess the advantage of using Sentinel-1 data in the detection of deforestation in the humid season, a multitemporal comparison was made between the deforestation detected with our method and the early warnings alerts ≥ 0.09 ha available in Geobosques. In this analysis, forest loss due to change in the course of rivers and false positives detected by our method were excluded.

Results

San Martin pilot area

Figure 9 shows the 82 deforestation polygons detected in the San Martin pilot area, of which 78 were correctly mapped and 4 were errors. The user's accuracy was 95.12%. To calculate producer's accuracy, 110 detections of early warnings alerts greater than 1ha available on the Geobosques platform were used, and a producer's accuracy of 70.91% was obtained (see table 4).

Table 4. Confusion matrix for the San Martin pilot area

Class	Number of Polygon			User's Accuracy
	Deforestation	No deforestation	Total	
Deforestation detected	78	4	82	95.12%
Reference data (Geobosques)	110	-	110	
Producer's Accuracy	70.91%			

The deforestation detected in the humid season is equivalent to 87.47 ha, and is mainly due to rice crops, that benefit from rainfall in the humid season. Deforestation detected in the dry season is equivalent to 57.67 ha.

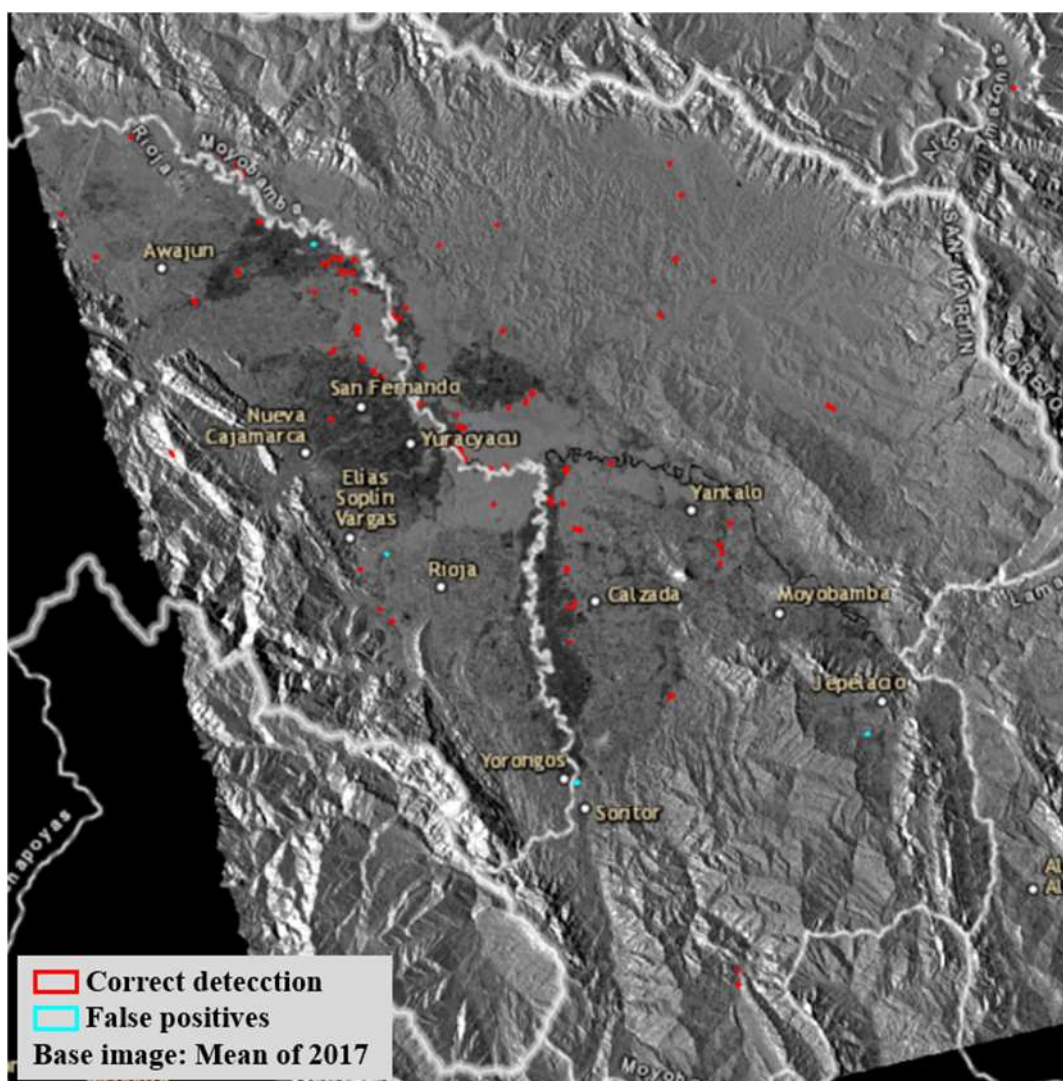


Figure 9. Correct deforestation polygons and the false positives in the San Martin pilot area, the base image corresponds to the mean of 2017 Sentinel-1 images.

Figure 10 shows the multitemporal comparison between the detected deforestation with Sentinel-1 and the early warnings alerts available in Geobosques. The new deforestation represents the percentage of deforestation that was only detected using Sentinel-1 and the percentage of coincidence shows the percentage of deforestation that matches the early warnings alerts available in Geobosques. In temporal series 1 (the dates of each temporal series are shown in table 3), 100% of the deforestation polygons detected with Sentinel-1 were not

detected with the early warnings alerts available in Geobosques. The coincidence was only 2.50% in the accumulated deforestation of series 1 and 2 and the coincidence was 10.38% in the case of accumulated deforestation of series 1 to 3, respectively. These temporal series correspond to the humid season and show the disadvantage of the optical systems when there is constant presence of clouds. In the cumulative deforestation from series 1 to 6, the coincidences were 44.00%. The low detection of the early warnings alerts available in Geobosques is due to the fact that the San Martin pilot area is located very close to mountainous areas, which means that the presence of clouds is also constant in the dry season.

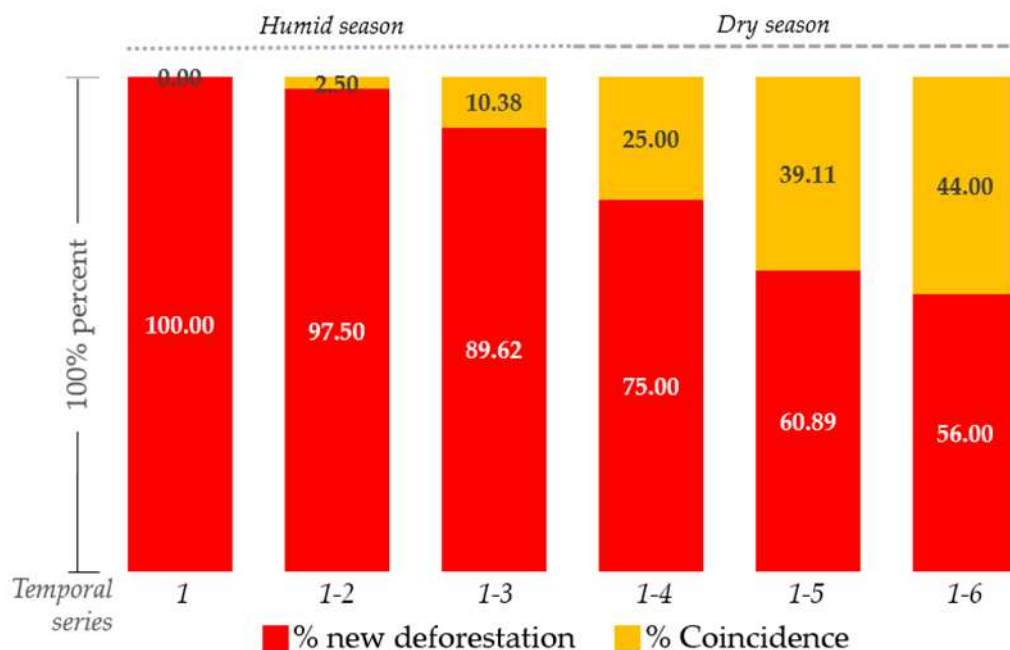


Figure 10. Multitemporal comparison of deforestation detected using Sentinel-1 and deforestation detected by the early warnings alerts available in Geobosques

Ucayali pilot area

582 deforestation polygons were detected in the Ucayali pilot area, of which 561 were correctly mapped and 21 were errors (see figure 11). The user’s accuracy was 96.39%. To calculate the producer’s accuracy, 1561 early warnings alerts greater than 1 ha available in the Geobosques platform were used, and an accuracy of 35.94% was obtained (see table 5).

Table 5. Confusion matrix for the Ucayali pilot area.

Class	Number of Polygon			User’s Accuracy
	Deforestation	No Deforestation	Total	
Deforestation detected	561	21	582	96.39%
Reference data (Geobosque)	1561	-	1561	
Producer’s Accuracy	35.94%			

556.08 ha were detected in the humid season and 1194.2 ha were detected in the dry season. This shows that the greatest deforestation occurs during the dry season, however, a significant level of deforestation was detected in the humid season.

The multitemporal comparison between the deforestation detected with Sentinel-1 and the early warnings alerts available in Geobosques are shown in figure 12. There was a coincidence of 50% in temporal series 1, 57.66% in temporal series 1 and 2 and 57.25% in the case of cumulative deforestation of temporal series 1 to 3, respectively. This percentage is higher than that obtained in the San Martin pilot area and is due to the fact that the Ucayali pilot area is more likely to have images with cloud free areas in the humid season (see table 7), and while approaching the dry season, the availability of images with low cloud percentage is greater. For this reason, a coincidence of 86.80% was obtained in the cumulative deforestation detected from series 1 to 6.

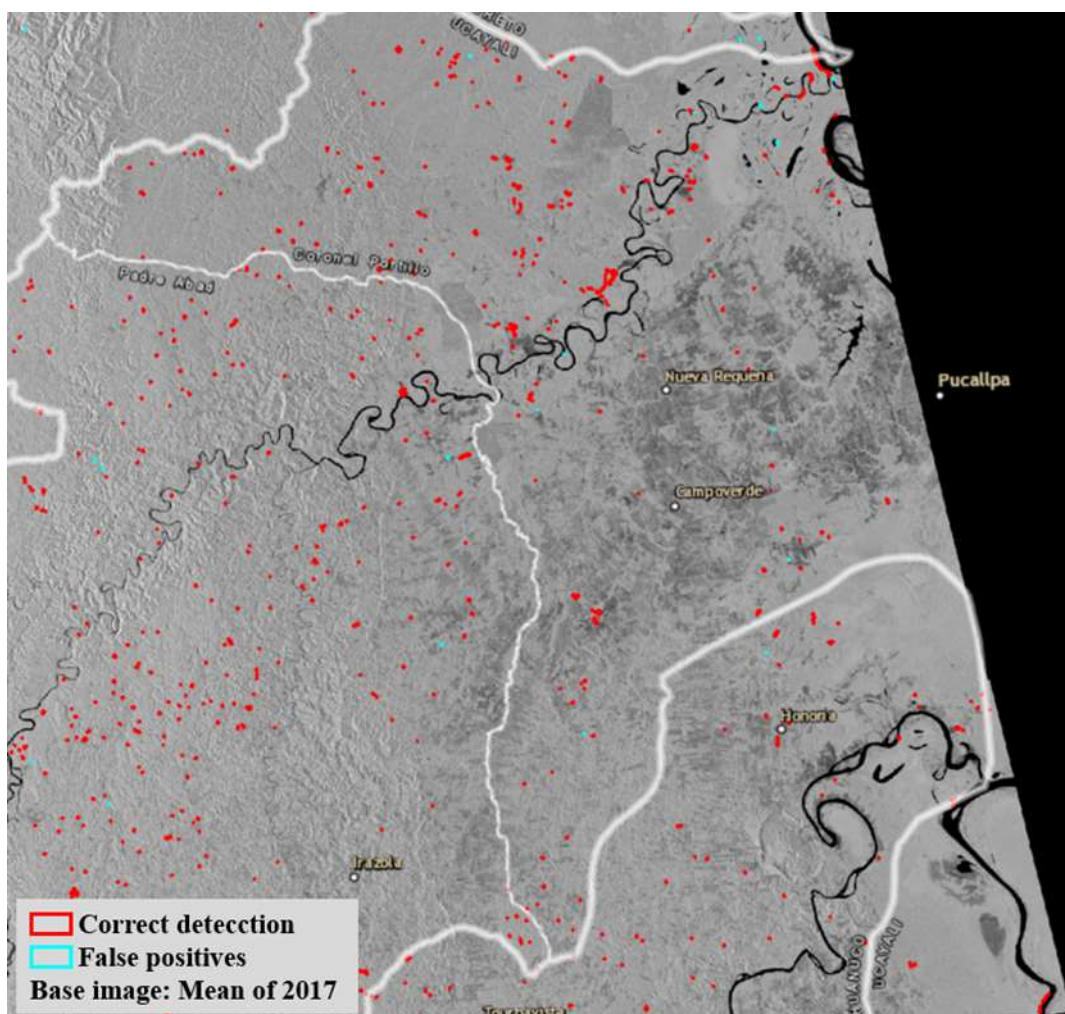


Figure 11. Correct deforestation polygons and the 21 false positives in the Ucayali pilot area, the base image corresponds to the mean of 2017 Sentinel-1 images.

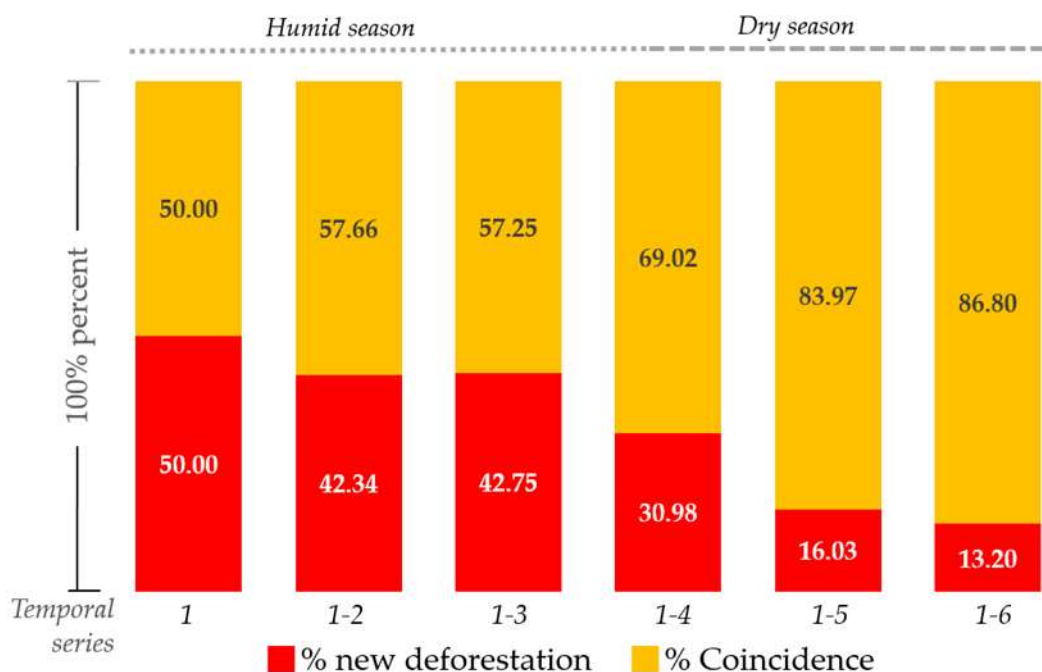


Figure 12. Multitemporal comparison of deforestation detected using Sentinel-1 and deforestation detected by the early warnings alerts available in Geobosques.

Madre de Dios pilot area

In the Madre de Dios pilot area, 909 deforestation polygons were correctly mapped and 20 were errors (see figure 13). The user's accuracy was 97.85%. To calculate the producer's accuracy, 1229 early warnings alerts greater than 1ha available in the Geobosques platform were used, and an accuracy of 73.96% was obtained (see Table 6).

Table 6. Confusion matrix for the Madre de Dios pilot area.

Class	Number of Polygon			User's Accuracy
	Deforestation	No Deforestation	Total	
Deforestation detected	909	20	929	97.85%
Reference data (Geobosques)	1229	-		
Producer's Accuracy	73.96%			

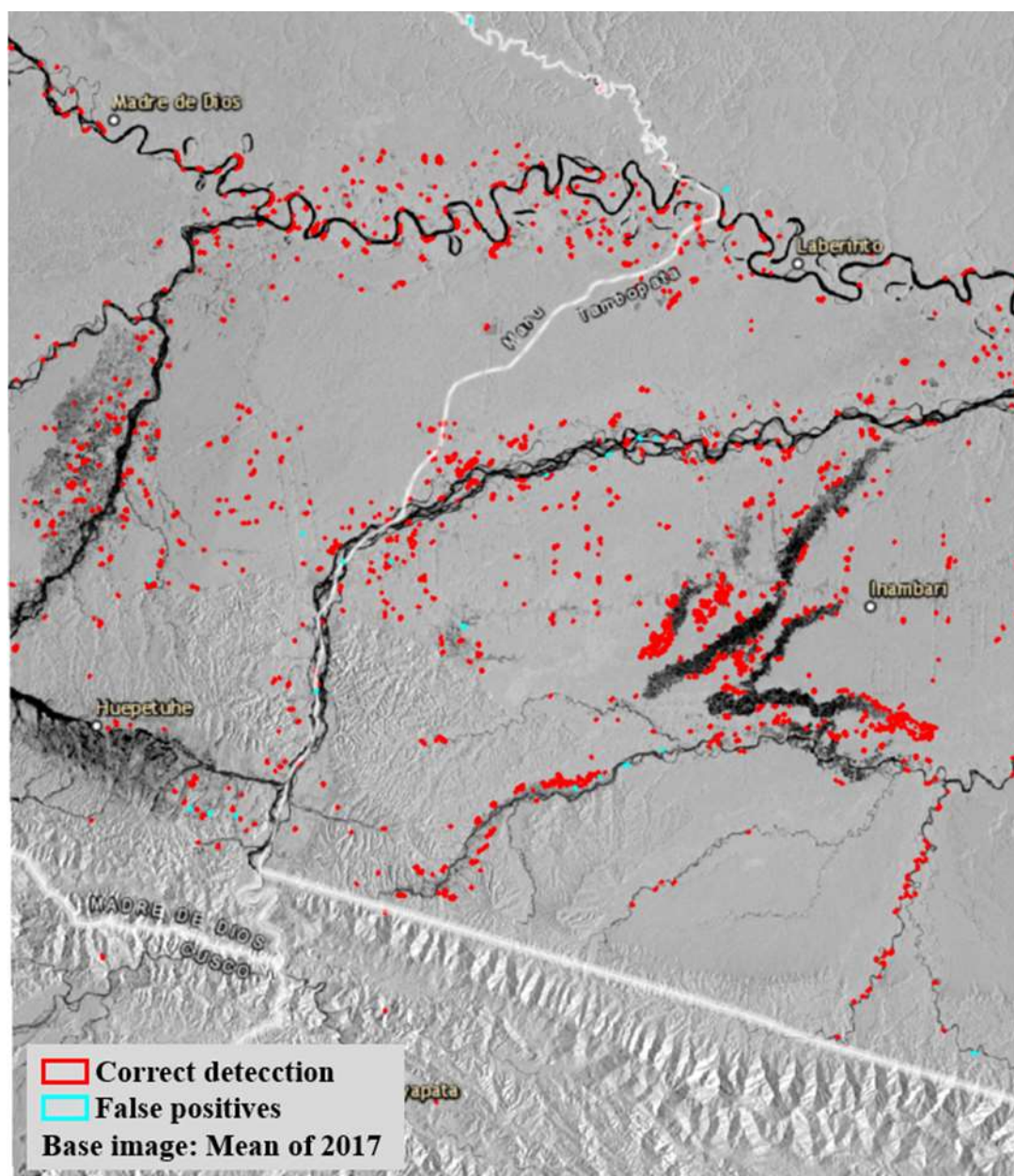


Figure 13. Correct deforestation polygons and the 20 false positives in the Madre de Dios pilot area, the base image corresponds to the mean of 2017 Sentinel-1 images.

The deforestation detected in the humid season is equivalent to 2054.96 ha and that detected in the dry season was 1968.08 ha.

The multitemporal comparison between the deforestation detected with Sentinel-1 and the early warnings alerts available in Geobosques. There was a coincidence of 46.42% in temporal series 1, 51.81% in the cumulative deforestation of temporal series 1 and 2 and 56.54% in the cumulative deforestation of series 1 to 3, respectively. These percentages are due to the fact that the probability of having cloud-free images is similar to the pilot area of Ucayali (see table 7). However, in the cumulative deforestation of series 1 to 4 and 1 to 5, the percentages of coincidence were 58.05% and 57.38% respectively; these percentages are lower than those obtained in the Ucayali pilot area. For the cumulative temporal series 1 to 6, the percentage of coincidences recently rose to 69.43% (see figure 14).

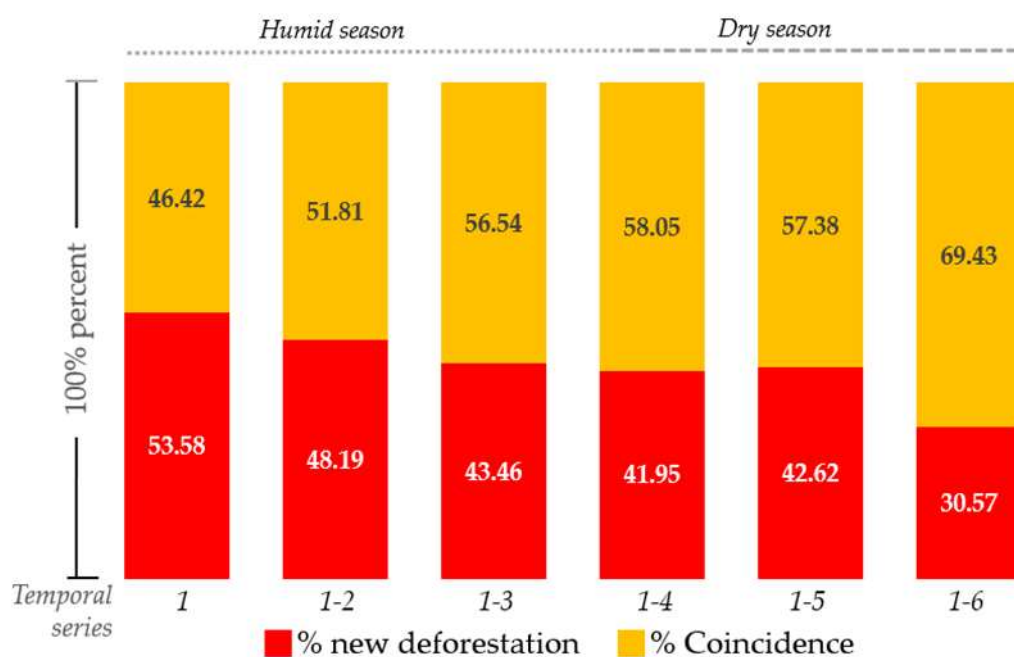


Figure 14. Multitemporal comparison of deforestation detected using Sentinel-1 and deforestation detected by the early warnings alerts available in Geobosques.

Discussion

The increased frequency of Sentinel-1 data allowed us to develop a simple methodology for the detection of deforestation every 36 days. In this study, we did not mix the data in ascending and descending orbital nodes, because the distortions that exist in mountainous areas (shadow, layover, foreshortening) seen from different orbits could generate false positives. However, our method was only applied to areas with slopes of less than 5°, so mixing data in ascending and descending orbital nodes is potentially feasible and could reduce the time span of detection to 18 days.

The choice of 1 ha as the minimum unit of mapping corresponds to the size that our main user (SERFOR) verifies and evaluates as the legal status of deforestation. Verifying deforestation in the dry season is a simple task because there is availability of optical images with a low percentage of clouds with which it is possible to examine whether deforestation is actually occurring. On the other hand, in the humid season, there are few good optical images available. In each case, the competent authorities have to invest time and money to send field brigades that can verify whether deforestation is actually occurring, so it is necessary to have deforestation data with high user's accuracy for an effective operation. Our methodology detects deforestation even under clouds with high user's accuracy of 96.45%, so that it can help the field operation significantly. If our minimum mapping unit was lower, then our user's accuracy would also be lower and we would deviate from the objectives of this work.

The producer's accuracies obtained in the three pilot areas were lower than its user's accuracies, due to the high presence of residues (trunks of trees, branches or bushes) in the deforested areas and the minimum mapping unit. The higher producer's accuracy in San Martin and Madre de Dios than that of Ucayali

because of a difference in the ground condition after deforestation. Deforested land in San Martin and Madre de Dios often turns into flooded lands (rice fields) and bare soil (illegal mining), which reflect less backscattering and therefore is easier to detect. On the other hand, in the Ucayali pilot area, deforestation leaves many residues on the surface and small scale deforestation (< 1 ha) is very frequent, causing much backscattering preventing deforestation detection. Figure 15 shows the backscattering behavior of 3 forest areas and their subsequent deforestation in the 6 time series. When the deforestation leaves soil without bare soil and/or bodies of water (for example, in the case of oil palm, illegal mining or rice fields), backscattering lowers considerably and its detection is simpler, but when deforestation leaves residues such as tree trunks, branches and shrubs, the backscattering generated by residues can be very similar to that of the forest, making it difficult to detect.

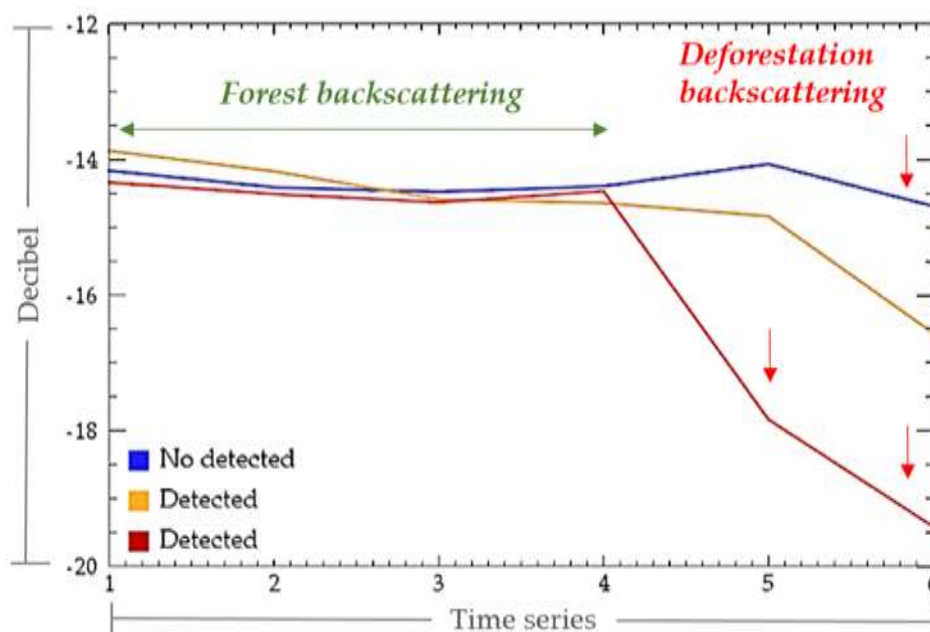


Figure 15. Backscattering of 3 deforested areas seen from the temporal series

Figure 16 (a) shows Sentinel-2 image dated 08/19/2018, where deforested areas are seen in light colors. Some of them could not be detected with our method due to the high presence of residues on the surface. For example, the deforestation patch found in the upper part could only be partially detected, and in the Sentinel-2 image, it can be seen that the part that could not be detected has the presence of green vegetation (possibly bushes). Figure 16 (b) shows an aerial photograph (GoPro camera) that corresponds to the partially detected deforestation patch. This photograph was taken on 10/03/2018 and shows that the area which cannot be detected has a darker color, due to the agglomeration of deforestation residues. Figure 16 (c) also shows deforested area that cannot be detected by our method. The aerial photography (GoPro camera) was taken on 10/03/2018 and it shows that these deforested areas have a high presence of deforestation residues agglomerated on the surface. If we modify the thresholds used for the detection of deforestation, we could detect this deforestation, but we would also have a greater presence of false positives and our user's accuracy would decrease.

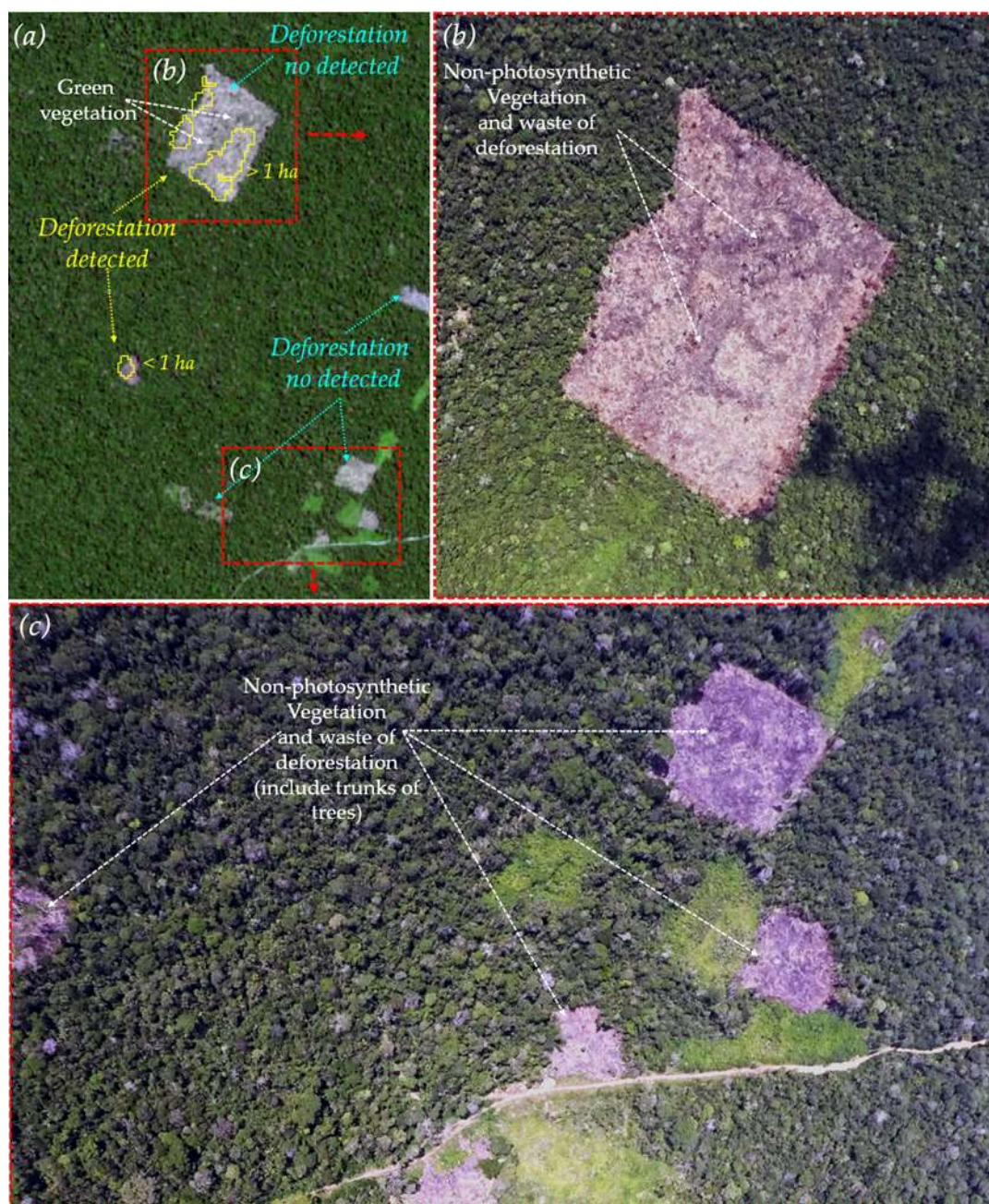


Figure 16. Deforested areas seen from the Sentinel-2 image dated 08/19/2018 (a) and aerial photograph taken with GoPro camera on 10/03/2018 (b, c).

In the three pilot areas, it was possible to detect deforestation that was not detected by the early warnings alerts of Geobosques. This shows the advantage of Sentinel-1 when there is the presence of clouds, especially in the humid season. Table 7 shows the cumulative monthly percentage of cloud free cover available in the images of the ETM+ and OLI sensors for the San Martín, Ucayali and Madre de Dios regions in 2018. The months with the highest presence of cloudiness are January, February, March, November and December. In these months, the use of Sentinel-1 would detect deforestation that otherwise wouldn't be detected by the early warnings alerts that use optical data. The synergies between both technologies is fundamental to have a robust monitoring of deforestation in the tropical humid forest of Peru.

Table 7. Cloud free cover in the images of the ETM+ and OLI sensors in 2018.

Month	San Martin	Ucayali	Madre de Dios
January	38.59%	11.63%	5.37%
February	8.28%	19.36%	17.21%
March	13.69%	32.63%	37.71%
April	52.54%	30.23%	63.24%
May	62.50%	63.08%	71.63%
June	87.88%	87.25%	92.18%
July	83.86%	94.87%	94.85%
August	79.94%	93.26%	93.15%
September	89.82%	97.14%	99.80%
October	46.13%	43.38%	73.80%
November	19.40%	2.96%	32.56%
December	25.75%	0.79%	31.09%

The high deforestation detected during the humid season in the Madre de Dios pilot area indicates that mining activities keeps going on throughout the humid season, and the early warning detection is essential to stop this activity, which in most cases is illegal. In this area, the data showed low correspondence with the early warnings from Geobosques for the dry season, in comparison with the results for the pilot area of Ucayali. For a better understanding of the evolution of the percentage of coincidences in the humid season, it was decided to verify on the platform <https://earthexplorer.usgs.gov/> the availability of ETM+ and OLI images with low percentage of clouds, between the dates: 05-08-2018 and 08-24-2018. Only 4 ETM+ and 2 OLI images had a cloud percentage lower than 30%. The pilot area is located between gaps of the ETM images, this explains the low level of coincidences that are found when the temporal series are included in the dry season.

Conclusions

The methodology developed allowed detection of deforestation events with more than 95% of user´s accuracy, which means that the data is reliable and could be used by any users monitoring forest.

Some of the deforestation events detected by our methodology were not detected by the early warnings of forest loss alerts that use Landsat data, mainly in the humid season. This is due to the advantages of SAR data in the humid season, and it is especially important in areas like Madre de Dios where deforestation caused by illegal mining must be detected quickly in order to stop deforestation before it causes more damage

This methodology will support the monitoring of deforestation in the tropical humid forests, providing a more robust monitoring.

Acknowledgments

The authors would like to thank JICA (Japan International Cooperation Agency). This study is based on one of the activities of the "Project on Capacity Development for Forest Conservation and REDD+ Mechanisms" in Peru (Probosque JICA Project) in 2016-2020. We also thank SERFOR for support of results validation and thank PNCBMCC for providing the Geobosques dataset.

References

1. MINAM, "Estrategia nacional sobre bosques y cambio climático," MINAM, Lima, Perú, 2016.
2. C. Vargas, Montalvan, Joselyn and A. León, "Early warning tropical forest loss alerts in Peru using Landsat," *Environmental Research Communications*, vol. 1, no. 12, 2019.
3. R. Peetersen, C. Davis, M. Herold and V. de Sy, "Tropical Forest Monitoring: Exploring the Gaps Between What is Required and What is Possible for REDD+ and Other Initiatives," Washington, D.C., USA, 2018.
4. C. M. Souza, S. Hayashi and A. Veríssimo, "Near real-time deforestation detection for enforcement of forest reserves in Mato Grosso," Washington DC, 2009.
5. L. Reymondin, A. Jarvis, A. Perez-Urbe, J. Touval, K. Argote, J. Rebetz, E. Guevara and M. Mulligan, "Terra-i: A methodology for near real-time monitoring of habitat change at continental scales using MODIS-NDVI and TRMM," *CIAT-Terra-i*, 2012.
6. D. Hammer, R. Kraft and D. Wheeler, "Alerts of forest disturbances from MODIS imagery," *International Journal of Applied Earth Observation and Geoinformation*, pp. 1-9, 2014.
7. D. Wheeler, B. Guzder-Williams, R. Petersen and D. Thau, "Rapid MODIS-based detection of tree cover loss," *International Journal of Applied Earth Observations and Geoinformation*, July 2018.
8. M. Hansen, A. Krylov, A. Tyukavina, P. Potapov, S. Turubanova, B. Zutta, I. Suspense, B. Margono, F. Stolle and R. Moore, "Humid tropical forest disturbance alerts using Landsat data," *Environmental Research Letters*, 2016.
9. J.-S. Lee and P. Eric, *Polarimetric Radar imaging from basic to applications*, Boca Raton, FL: Taylor y Francis Group, 2009.
10. R. Almeida-Filho, A. Rosenqvist, Y. Shimabukuro and R. Silva-Gomez, "Detecting deforestation with multitemporal L-Band SAR imagery: a case study in western Brazilian Amazônia," *International Journal of Remote Sensing*, vol. 28, no. 6, pp. 1383-1390, 2007.
11. M. M. Rahman and J. T. Sumantyo, "Mapping tropical forest cover and deforestation using synthetic aperture radar (SAR) images," *Applied Geomatics*, 2010.
12. F. Chen, N. Ishwaran and J. C. Brito, "Deforestation monitoring in the Amazon River estuary by multi-temporal Envisar ScanSAR data," in *IOP Conference Series: Earth and Environmental Science*, 2016.
13. H. N. Mesquita Jr, C. Dupas, M. C. Silva and D. M. Valeriano, "Amazon deforestation monitoring system with ALOS SAR complementary data," in *The International Archives of the Photogrammetry, Remote Sensing and Spatial Information Sciences*, Beijing, 2008.
14. T. Motohka, M. Shimada, Y. Uryu and S. Budi, "Using time series PALSAR gamma nought mosaics for automatic detection of tropical deforestation: A test study in Riau, Indonesia," *Remote Sensing of Environment*, vol. 155, pp. 79-88, 2014.
15. A. Bouvet, S. Mermoz, M. Ballere, T. Koleck and T. Le Toan, "Use of the SAR Shadowing Effect for Deforestation Detection with Sentinel-1 Time Series," *Remote Sensing*, vol. 10, no. 8, 2018.
16. J. Reiche, S. Bruin, D. Hoekman, J. Verbesselt and M. Herold, "A Bayesian Approach to Combine Landsat and ALOS PALSAR Time Series for Near Real-Time Deforestation Detection," *Remote Sensing*, vol. 7, no. 5, pp. 4973-4996, 2015.
17. J. Reiche, J. Verbesselt, D. Hoekman and M. Herold, "Fusing Landsat and SAR time series to detect deforestation in the tropics," *Remote Sensing of Environment*, vol. 156, pp. 276-293, 2015.
18. J. Reiche, E. Hamunyela, J. Verbesselt, D. Hoekman and M. Herold, "Improving near-real time deforestation monitoring in tropical dry forests by combining dense Sentinel-1 time series with Landsat and ALOS-2 PALSAR-2," *Remote Sensing of Environment*, vol. 204, pp. 147-161, January 2018.
19. M. Watanabe, C. Koyama, M. Hayashi, I. Nagami, T. Tadono and M. Shimada, "Semi-Automatic deforestation detection algorithm with Palsar-2/ScanSAR HH/HV Polarizations," in *IGARSS 2018 - International Geoscience and Remote Sensing Symposium*, Valencia, 2018.

20. JJ-FAST, 22 11 2018. [Online]. Available: <https://www.eorc.jaxa.jp/jjfast/system.html>. [Accessed 22 11 2018].
21. M. Watanabe, C. Koyama, M. Hayashi, I. Nagatani and M. Shimada, "Early-Stage Deforestation Detection in the Tropics with L-Band SAR," *IEEE journal of selected topics in applied earth observations and remote sensing*, vol. 11, no. 6, June 2018.
22. "GEOBOSQUES," Noviembre 2018. [Online]. Available: <http://geobosques.minam.gob.pe/geobosque/view/perdida.php>.
23. J. Reiche, R. Verhoeven, J. Verbesselt, E. Hamunyela, N. Wielaard and M. Herold, "Characterizing tropical forest cover loss using dense Sentinel-1 data and active fire alerts," *Remote Sensing*, vol. 10, no. 5, 2018.
24. M. Hirschmugl, J. Deutscher, C. Sobe, A. Bouvet, S. Mermoz and M. Schardt, "Use of SAR and Optical Time Series for Tropical Forest Disturbance Mapping," *Remote Sensing*, vol. 12, no. 4, 2020.
25. K. Shimizu, T. Ota and N. Mizoue, "Detecting Forest Changes Using Dense Landsat 8 and," *Remote Sensing*, vol. 11, no. 1899, 2019.
26. M. J. Weisse, R. Nogueroń, R. E. Vivanco and D. Castillo, "Use of Near-Real-Time deforestation alerts: A case study from Peru," October 2019. [Online]. Available: <https://www.wri.org/publication/use-near-real-time-deforestation-alerts>.
27. MINAM, "Memoria Descriptiva del Mapa de Cobertura Vegetal del Perú," MINAM, Lima, 2012.
28. PNCBMCC, "Boletín de Alertas Tempranas de Deforestación (ATD) 1," MINAM, 2018.
29. J. Caballero, M. Messinger, F. Román-Dañobeytia, C. Ascorra, L. E. Fernandez and M. Silman, "Deforestation and Forest Degradation Due to Gold Mining in the Peruvian Amazon: A 34-Year Perspective," *Remote Sensing*, vol. 10, no. 1903, 2018.
30. G. P. Asner and R. Tupayachi, "Accelerated losses of protected forests from gold mining in the Peruvian Amazon," *Environmental Research Letters*, vol. 12, no. 9, 2016.
31. ESA, "Sentinel-1 SAR Technical Guide," ESA, 2018. [Online]. Available: <https://sentinel.esa.int/web/sentinel/technical-guides/sentinel-1-sar>. [Accessed diciembre 2018].
32. Google, "Sentinel-1 Algorithms," 15 Agosto 2018. [Online]. Available: <https://developers.google.com/earth-engine/sentinel1>. [Accessed Diciembre].
33. Z. Shi and K. B. Fung, "A comparison of digital speckle filters," in *Proceedings of IGARSS 94 - 1994 IEEE International Geoscience and Remote Sensing Symposium*, 1994.
34. W. Manabu, C. Koyama, M. Hayashi, I. Nagatani, T. Tadono and M. Shimada, "Semi-automatic deforestation detection algorithm with Palsar-2/ScanSAR HH/HV Polarizations," in *Proceedings of IGARSS 2018 - 2018 IEEE International Geoscience and Remote Sensing Symposium*, 2018.
35. N. Joshi, E. T. Mitchard, N. Woo, J. Torres, J. Moll-Rocek, A. Ehammer, M. Collins, M. R. Jepsen and R. Fensholt, "Mapping dynamics of deforestation and forest degradation in tropical forest using radar satellite data," *Environmental Research Letters*, vol. 10, no. 3, 2015.
36. R. Almeida-Filho, Y. E. Shimabukuru, A. Rosenqvist and G. A. Sanchez, "Using dual-polarized alos palsar data for detecting new fronts of deforestation in the Brazilian Amazônia," *International Journal of Remote Sensing*, vol. 30, no. 14, pp. 3735-3743, 2009.